

Light trapping in thin-film solar cells with randomly rough and hybrid textures

Piotr Kowalczewski,* Marco Liscidini, and Lucio Claudio Andreani

Department of Physics, University of Pavia, Via Bassi 6, I-27100 Pavia, Italy

*piotr.kowalczewski@unipv.it

Abstract: We study light-trapping in thin-film silicon solar cells with rough interfaces. We consider solar cells made of different materials (c-Si and μ c-Si) to investigate the role of *size* and *nature* (direct/indirect) of the energy band gap in light trapping. By means of rigorous calculations we demonstrate that the Lambertian Limit of absorption can be obtained in a structure with an optimized rough interface. We gain insight into the light trapping mechanisms by analysing the optical properties of rough interfaces in terms of Angular Intensity Distribution (AID) and haze. Finally, we show the benefits of merging ordered and disordered photonic structures for light trapping by studying a hybrid interface, which is a combination of a rough interface and a diffraction grating. This approach gives a significant absorption enhancement for a roughness with a modest size of spatial features, assuring good electrical properties of the interface. All the structures presented in this work are compatible with present-day technologies, giving recent progress in fabrication of thin monocrystalline silicon films and nanoimprint lithography.

© 2013 Optical Society of America

OCIS codes: (040.5350) Photovoltaic; (050.1950) Diffraction gratings; (240.0310) Thin films; (240.5770) Roughness.

References and links

1. H. Tan, R. Santbergen, A. H. M. Smets, and M. Zeman, "Plasmonic light trapping in thin-film silicon solar cells with improved self-assembled silver nanoparticles," *Nano Lett.* **12**, 4070–4076 (2012).
2. S. Morawiec, M.J. Mendes, S. Mirabella, F. Simone, F. Priolo, and I. Crupi, "Self-assembled silver nanoparticles for plasmon-enhanced solar cell back reflectors: correlation between structural and optical properties," *Nanotechnology* **24**, 265601 (2013).
3. A. Bozzola, M. Liscidini, and L. C. Andreani, "Photonic light-trapping versus Lambertian limits in thin film silicon solar cells with 1D and 2D periodic patterns," *Opt. Express* **20**, A224–A244 (2012).
4. O. Isabella, S. Solntsev, D. Caratelli, and M. Zeman, "3-D optical modeling of thin-film silicon solar cells on diffraction gratings," *Prog. Photovolt: Res. Appl.* **21**, 94–108 (2013).
5. C. S. Schuster, P. Kowalczewski, E. R. Martins, M. Patrini, M. G. Scullion, M. Liscidini, L. Lewis, C. Reardon, L.C. Andreani, and T.F. Krauss, "Dual gratings for enhanced light trapping in thin-film solar cells by a layer-transfer technique," *Opt. Express* **21**, A433–A439 (2013).
6. C. Martella, D. Chiappe, P. Delli Veneri, L.V. Mercaldo, I. Usatii, and F. Buatier de Mongeot, "Self-organized broadband light trapping in thin film amorphous silicon solar cells," *Nanotechnology* **24**, 225201 (2013).
7. M. Burrese, F. Pratesi, K. Vynck, M. Prasciolu, M. Tormen, and D. S. Wiersma, "Two-dimensional disorder for broadband, omnidirectional and polarization-insensitive absorption," *Opt. Express* **21**, A268–A275 (2013).
8. R. Dewan, J. I. Owen, D. Madzharov, V. Jovanov, J. Hüpkens, and D. Knipp, "Analyzing nanotextured transparent conductive oxides for efficient light trapping in silicon thin film solar cells," *Appl. Phys. Lett.* **101**, 103903 (2012).

9. T. Lanz, B. Ruhstaller, C. Battaglia, and C. Ballif, "Extended light scattering model incorporating coherence for thin-film silicon solar cells," *J. Appl. Phys.* **110**, 033111 (2011).
10. S. Wiesendanger, M. Zilk, T. Pertsch, C. Rockstuhl, and F. Lederer, "Combining randomly textured surfaces and photonic crystals for the photon management in thin film microcrystalline silicon solar cells," *Opt. Express* **21**, A450–A459 (2013).
11. Z. Yu, A. Raman, and S. Fan, "Fundamental limit of light trapping in grating structures," *Opt. Express* **18**, A366–A380 (2010).
12. I. Simonsen, "Optics of surface disordered systems," *Eur. Phys. J. — Special Topics* **181**, 1–103 (2010).
13. S. Fahr, T. Kirchartz, C. Rockstuhl, and F. Lederer, *Opt. Express* **19**, A865–A874 (2011).
14. K. Jäger, M. Fischer, R. A. C. M. M. van Swaaij, and M. Zeman, "A scattering model for nano-textured interfaces and its application in opto-electrical simulations of thin-film silicon solar cells," *J. Appl. Phys.* **111**, 083108 (2012).
15. K. Jäger, M. Fischer, R. A. C. M. M. van Swaaij, and M. Zeman, "Designing optimized nano textures for thin-film silicon solar cells," *Opt. Express* **21**, A656–A668 (2013).
16. P. Kowalczewski, M. Liscidini, and L. C. Andreani, "Engineering Gaussian disorder at rough interfaces for light trapping in thin-film solar cells," *Opt. Lett.* **37**, 4868–4870 (2012).
17. C. Rockstuhl, S. Fahr, K. Bittkau, T. Beckers, R. Carius, F.-J. Haug, T. Söderström, C. Ballif, and F. Lederer, "Comparison and optimization of randomly textured surfaces in thin-film solar cells," *Opt. Express* **18**, A335–A341 (2010).
18. V. Depauw, Y. Qiu, K. Van Nieuwenhuysen, I. Gordon, and J. Poortmans, "Epitaxy-free monocrystalline silicon thin film: first steps beyond proof-of-concept solar cells," *Progr. Photovolt: Res. Appl.* **19**, 844–850 (2011).
19. X. Meng, V. Depauw, G. Gomard, O. El Daif, C. Trompoukis, E. Drouard, C. Jamois, A. Fave, F. Dross, I. Gordon, and C. Seassal, "Design, fabrication and optical characterization of photonic crystal assisted thin film monocrystalline-silicon solar cells," *Opt. Express* **20**, A465–A475 (2012).
20. C. Trompoukis, O. El Daif, V. Depauw, I. Gordon, and J. Poortmans, "Photonic assisted light trapping integrated in ultrathin crystalline silicon solar cells by nanoimprint lithography," *Appl. Phys. Lett.* **101**, 103901 (2012).
21. C. Battaglia, J. Escarré, K. Söderström, L. Erni, L. Ding, G. Bugnon, A. Billet, M. Boccard, L. Barraud, S. De Wolf, F.-J. Haug, M. Despeisse, and C. Ballif, "Nanoimprint Lithography for High-Efficiency Thin-Film Silicon Solar Cells," *Nano Lett.* **11**, 661–665 (2011).
22. V. Freilikher, E. Kanziiper, and A. Maradudin, "Coherent scattering enhancement in systems bounded by rough surfaces," *Phys. Rep.* **288**, 127–204 (1997).
23. D. M. Whittaker and I. S. Culshaw, "Scattering-matrix treatment of patterned multilayer photonic structures," *Phys. Rev. B* **60**, 2610–2618 (1999).
24. M. Liscidini, D. Gerace, L. C. Andreani, and J. E. Sipe, "Scattering-matrix analysis of periodically patterned multilayers with asymmetric unit cells and birefringent media," *Phys. Rev. B* **77**, 035324 (2008).
25. E.D. Palik, *Handbook of Optical Constants of Solids* (Academic, Orlando, 1985).
26. K. H. Jun, R. Carius, and H. Stiebig, "Optical characteristics of intrinsic microcrystalline silicon," *Phys. Rev. B* **66**, 115301 (2002).
27. Reference Solar Spectral Irradiance: Air Mass 1.5, <http://rredc.nrel.gov/solar/spectra/am1.5/>.
28. J. Nelson, *The Physics of Solar Cells* (Imperial College Press, London, 2003).
29. D. Gerace and L. C. Andreani, "Disorder-induced losses in photonic crystal waveguides with line defects," *Opt. Lett.* **29**, 1897–1899 (2004).
30. D. Gerace and L. C. Andreani, "Low-loss guided modes in photonic crystal waveguides," *Opt. Express* **13**, 4939–4951 (2005).
31. S. Hughes, L. Ramunno, J. F. Young, and J. E. Sipe, "Extrinsic optical scattering loss in photonic crystal waveguides: Role of fabrication disorder and photon group velocity," *Phys. Rev. Lett.* **94**, 033903 (2005).
32. E. Yablonovitch, "Statistical ray optics," *J. Opt. Soc. Am.* **72**, 899–907 (1982).
33. M. A. Green, "Lambertian light trapping in textured solar cells and light-emitting diodes: analytical solutions," *Prog. Photovolt: Res. Appl.* **10**, 235–241 (2002).
34. A. Bozzola, M. Liscidini, and L. C. Andreani, "Broadband light trapping with disordered photonic structures in thin-film silicon solar cells," *Prog. Photovolt: Res. Appl.* (2013). In press, published online: <http://dx.doi.org/10.1002/pip.2385>.
35. J. Krč, M. Zeman, O. Kluth, F. Smole, and M. Topič, "Effect of surface roughness of ZnO:Al films on light scattering in hydrogenated amorphous silicon solar cells," *Thin Solid Film* **426**, 296–304 (2003).
36. E. Forniés, C. Zaldo, and J. M. Albella, "Control of random texture of monocrystalline silicon cells by angle-resolved optical reflectance," *Sol. Energ. Mat. Sol. Cells* **87**, 583–593 (2005).
37. J. Escarré, K. Söderström, M. Despeisse, S. Nicolay, C. Battaglia, G. Bugnon, L. Ding, F. Meillaud, F.-J. Haug, and C. Ballif, "Geometric light trapping for high efficiency thin film silicon solar cells," *Sol. Energ. Mat. Sol. Cells* **98**, 185–190 (2012).
38. M. Python, E. Vallat-Sauvain, J. Bailat, D. Dominé, L. Fesquet, A. Shah, and C. Ballif, "Relation between substrate surface morphology and microcrystalline silicon solar cell performance," *J. Non-Cryst. Solids* **354**, 2258–2262 (2008).

39. C. Battaglia, C.-M. Hsu, K. Söderström, J. Escarré, F.-J. Haug, M. Charrière, M. Boccard, M. Despeisse, D. T. L. Alexander, M. Cantoni, Y. Cui, and C. Ballif, "Light trapping in solar cells: Can periodic beat random?," *ACS Nano* **6**, 2790–2797 (2012).
 40. O. Isabella, F. Moll, J. Krč, and M. Zeman, "Modulated surface textures using zinc-oxide films for solar cells applications," *Phys. Status Solidi A* **207**, 642–646 (2010).
 41. K. Vynck, M. Burrese, F. Riboli, and D.S. Wiersma, "Photon management in two-dimensional disordered media," *Nat. Mater.* **11**, 1017–1022 (2012).
 42. M. Boccard, C. Battaglia, S. Hänni, K. Söderström, J. Escarré, S. Nicolay, F. Meillaud, M. Despeisse, and C. Ballif, "Multiscale transparent electrode architecture for efficient light management and carrier collection in solar cells," *Nano Lett.* **12**, 1344–1348 (2012).
-

1. Introduction

Strong and broad-band light trapping is necessary to obtain highly efficient thin-film solar cells, thus a number of different light-management strategies have been explored, including plasmonic nanoparticles [1, 2], ordered [3–5] and disordered [6–9] photonic structures, as well as combinations of both [10]. These studies show that although ordered photonic structures can give a significant absorption enhancement, this is often limited to narrow wavelength intervals [11]. It is also known that a broad-band absorption enhancement requires photonic structures with a certain amount of disorder. For this reason, randomly rough interfaces [12–15], being intrinsically broad-band scatterers, are particularly promising. Yet, the description of a realistic rough surface topography is complicated, which makes the study and the optimization of light-trapping a challenging task.

In our previous work [16], we have presented a one-dimensional model of randomly rough Gaussian surface that is able to describe the optical properties of state-of-the-art rough substrates (e.g., Neuchâtel and Asahi-U) by means of only two statistical parameters: the root mean square deviation of height and the lateral correlation length. Scattering properties of two-dimensional random surfaces can be investigated using one-dimensional model because optical response of considered substrates is isotropic. In particular, we performed the calculations for unpolarized light (i.e., average of both polarizations) and took an average of the results obtained for an ensemble of one-dimensional rough surface realizations. By comparison with rigorous simulations of real two-dimensional substrates [17], we have shown [16] that this simple approach gives accurate results without being computationally too demanding.

In this contribution, we use the same model to further investigate light-trapping in thin-film silicon solar cells with rough interfaces. In particular, we focus on solar cells made of different materials, to determine the role of *size* and *nature* (direct/indirect) of the energy band gap in light trapping. We demonstrate that the Lambertian limit of absorption can be obtained in a structure with an optimized roughness. Analysis of the optical properties of rough interfaces, in terms of haze and Angular Intensity Distribution (also called Angle-Resolved Scattering or Angular Distribution Function), gives insight into the light trapping mechanisms. Finally, we explore the concept of a hybrid interface, which is a combination of a rough interface and a diffraction grating. We show that this approach can give a significant absorption enhancement for a roughness with a modest size of spatial features, and it can be of help in maintaining good electrical properties of the interface.

In this work, we focus on crystalline (c-Si) and microcrystalline (μ c-Si) silicon solar cells. Epitaxy-free fabrication of thin monocrystalline silicon films and solar cells [18–20] and the ability of the roughness model to describe realistic rough surface topographies suggest that practical realizations of the considered structures are compatible with current technologies. Moreover, nanoimprint lithography allows fabrication of random textures on a large area and at low costs [21].

This paper is organized as follows: The model of roughness and our numerical approach

are summarized in Sec. 2. In Sec. 3, we discuss randomly rough textures for light trapping in c-Si and μ c-Si solar cells. In Sec. 4, we evaluate the optical performance of solar cells with optimized random interfaces, by comparing it with the corresponding Lambertian Limit. Sec. 5 gives insight into the optical properties of rough textures by means of Angular Intensity Distribution and haze. Finally, in Sec. 6, we consider the hybrid texture, showing the benefits of combining a randomly rough interface with an ordered photonic structure.

2. Model of roughness and numerical approach

For the sake of completeness, this section gives a general description of the model of roughness and of our numerical approach. More details, as well as the results of the validation of the model, can be found in [16].

In our approach, we consider a one-dimensional interface with a Gaussian roughness, described by the vertical root mean square (RMS) deviation of height σ and the lateral correlation length l_c , which is proportional to the average spacing between consecutive minima/maxima of the rough interface. The algorithm used to generate randomly rough interfaces with a given σ and l_c was taken from [22].

The calculations of the optical properties of measured rough surface topographies, reported in [17], provided a benchmark to validate our approach. First, we used the RMS of height and the lateral correlation length of Neuchâtel and Asahi-U substrates as input parameters to the one-dimensional model of Gaussian roughness. By Rigorous Coupled-Wave Analysis (RCWA) [23, 24], we calculated the scattering properties of both interfaces, namely the haze and the Angular Intensity Distribution of the transmitted light. Second, we compared our results with the haze and the AID documented in [17], which were calculated for the two-dimensional measured surface topographies. The comparison gave a surprisingly good agreement, which confirms that this 1D model of Gaussian roughness provides an accurate description of the optical properties of 2D realistic surface topographies.

It is important to note that in our approach we have been able to reduce the dimensionality of the problem without a loss of accuracy, because the scattering properties of rough interfaces are isotropic. This step allowed to drastically decrease the computational cost.

The solar cells investigated here are sketched in Fig. 1. The structures consist of crystalline [25] or microcrystalline [26] silicon absorber, anti-reflection coating (ARC), and a silver [25]

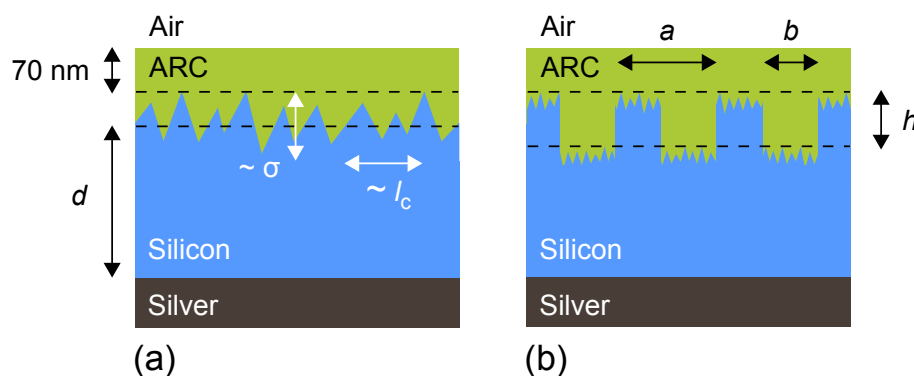


Fig. 1. Structures under consideration: (a) thin-film silicon solar cell with the randomly rough interface, described by the RMS of height σ and the lateral correlation length l_c ; (b) thin-film silicon solar cell with the hybrid interface, being a combination of a rough interface and a diffraction grating. The grating has period a , width of the etched region b , and etching depth h .

back reflector. The ARC is taken transparent, with refractive index equal to $n_{\text{ARC}}=1.65$ and thickness equal to 70 nm, which was found to be optimal (within ± 5 nm) for both materials. For different parameters of the roughness, the volume of silicon is kept constant, and it corresponds to the structure with a flat ARC/Si interface. The only difference between the two structures is the ARC/Si interface, which is the randomly rough texture in Fig. 1(a), or the combination of rough interface and a diffraction grating in Fig. 1(b).

The optical properties of the solar cells are modelled by RCWA, with rough interfaces described by the staircase approximation. The period of the computational cells is taken equal to $10\ \mu\text{m}$, much larger than the lateral correlation length of the roughness, which allows to neglect the effects of periodicity. Finally, all the calculations are performed for unpolarized light.

We use the short-circuit current density J_{SC} calculated for the AM1.5G [27] spectrum as the figure of merit. In our analysis, we do not consider the electrical properties of the solar cells, assuming unity electron-hole pair collection efficiency. J_{SC} is thus expressed as [28]:

$$J_{\text{SC}} = q \int b_{\text{S}}(E)A(E)dE, \quad (1)$$

where b_{S} is the incident solar photon flux density (number of photons per unit area and per unit time in the energy interval dE around E) and $A(E)$ is the absorbance in the active layer. For both c-Si and $\mu\text{c-Si}$, integration is done for the energy window between 1.1 and 4.2eV.

3. Randomly rough textures for light trapping in c-Si and $\mu\text{c-Si}$ solar cells

First, we consider the solar cell sketched in Fig. 1(a), with $\mu\text{c-Si}$ absorbing layer of $1\ \mu\text{m}$. In Fig. 2 we show the short-circuit current density calculated as a function of l_{c} , from 60 to 220 nm, and σ , from 0 to 300 nm. Each point is calculated as an average of 10 surface realizations. The J_{SC} mainly depends on σ , with a modest, in this parameter range, bell-like dependence on l_{c} . These trends are similar to the results for the crystalline silicon solar cell reported in [16].

To explore the difference in the optical performance between c-Si and $\mu\text{c-Si}$ solar cells with rough interfaces, we calculated the short-circuit current density as a function of σ at fixed $l_{\text{c}} = 160\text{nm}$, being the optimal value for both materials. The results, shown in Fig. 3, revealed that for the flat structure, or when the roughness is small, absorption in the c-Si solar cell (indirect band gap) is lower than absorption in the $\mu\text{c-Si}$ solar cell (quasi-direct band gap). Yet, when the roughness is large enough, the c-Si structure outperforms the one made of $\mu\text{c-Si}$. These results lead to the conclusion that without light trapping, absorption in the structure is mainly determined by the *nature* (direct/indirect) of the band gap. For an efficient light trapping, however, the band gap *size* is the most important, and materials with a smaller band gap can give a higher absorption.

As already observed in [16], J_{SC} decreases for small σ . In this range, the effective thickness of the ARC is no longer optimal, and, at the same time, the roughness is too small to provide an efficient anti-reflection action. The J_{SC} for the flat structure with a non-optimal ARC is smaller than in the structure with the optimized ARC, and it increases quadratically at small σ . This is an analogy to the scattering losses in photonic crystal waveguides in the perturbative regime [29–31]. Finally, for σ larger than few tens of nanometres, the AR action is almost entirely performed by the roughness, which is large enough to prevent a constructive interference in the ARC. Therefore, for large σ , the ARC only smooths the transition between the refractive indices of air and silicon.

To explain why c-Si solar cell outperforms the one made of $\mu\text{c-Si}$ when light trapping is efficient enough, in Fig. 4 we compare the absorption and the corresponding spectral contribution to the short-circuit current density dJ_{SC}/dE in c-Si and $\mu\text{c-Si}$ solar cells, at three different values of σ . With increasing σ , dJ_{SC}/dE in the c-Si cell gradually exceeds the one in the $\mu\text{c-Si}$

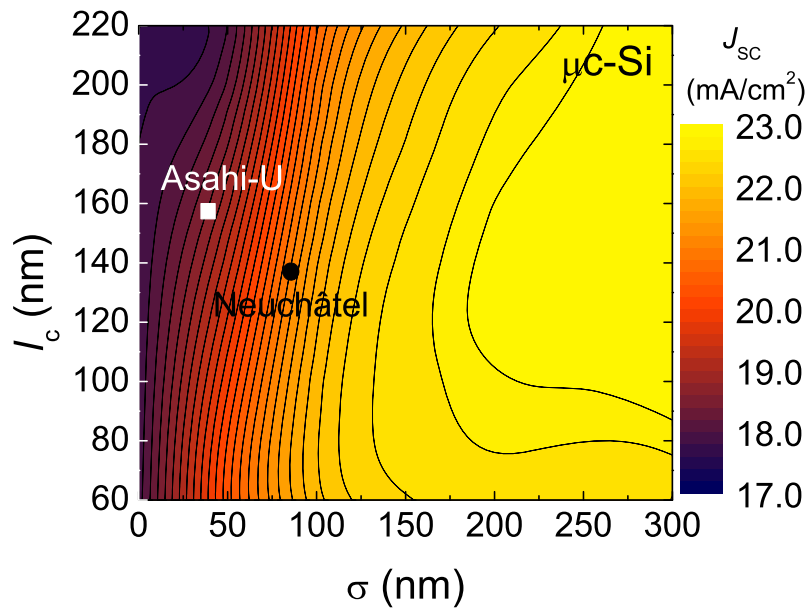


Fig. 2. Short-circuit current density as a function of lateral correlation length l_c and RMS deviation of height σ , for a $1\ \mu\text{m}$ thick $\mu\text{c-Si}$ solar cell with rough interface. Each point is calculated as an average of 10 surface realizations.

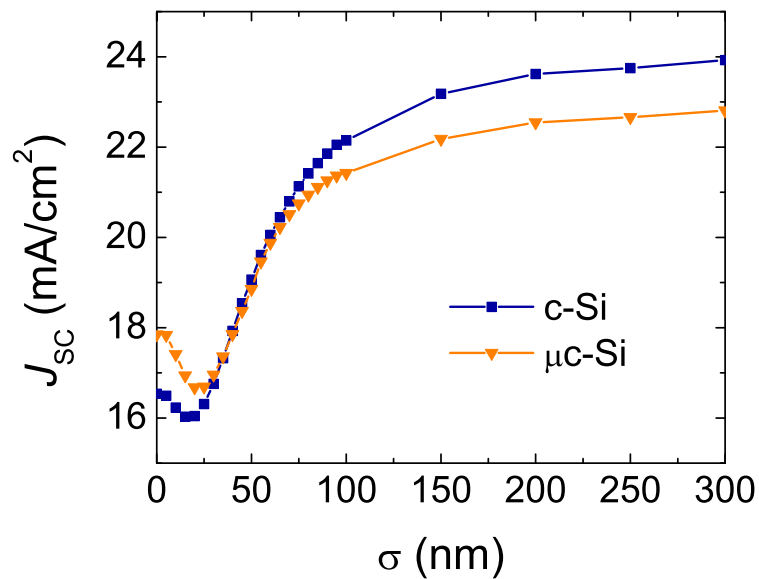


Fig. 3. Short-circuit current density as a function of RMS deviation of height σ , for $1\ \mu\text{m}$ thick c-Si and $\mu\text{c-Si}$ solar cells with rough interfaces. Lateral correlation length is equal to $l_c = 160\ \text{nm}$.

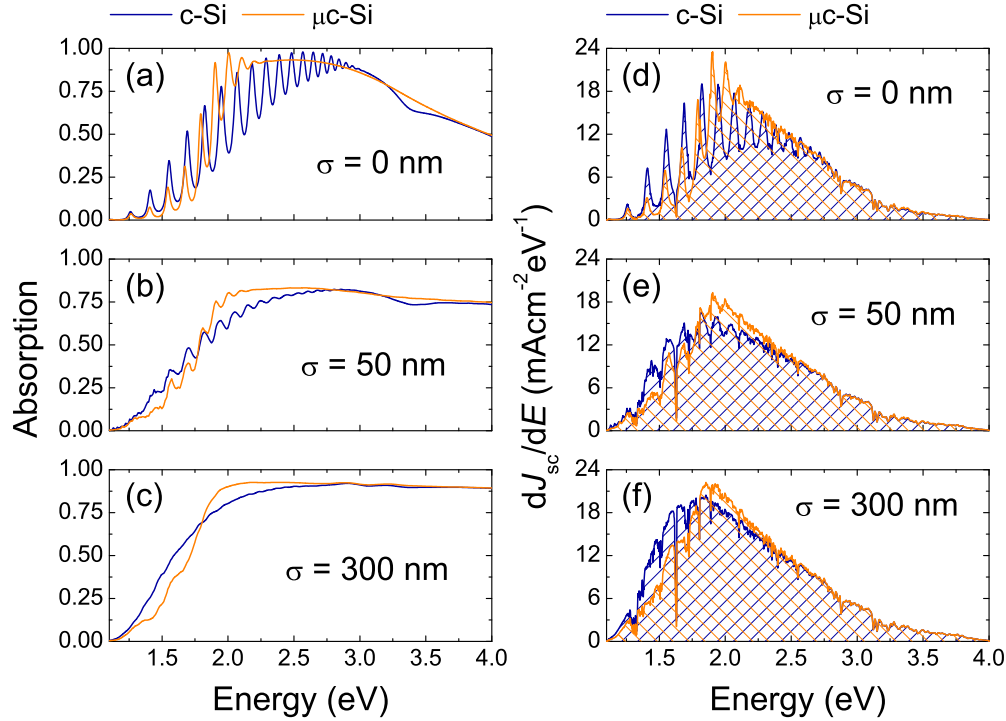


Fig. 4. Absorption (left) and spectral contribution to the short-circuit current density (right) in $1\ \mu\text{m}$ -thick c-Si and $\mu\text{c-Si}$ solar cells, at three different values of RMS deviation of height σ . Lateral correlation length is equal to $l_c = 160\ \text{nm}$.

cell. Finally, for $\sigma = 300\ \text{nm}$ (Fig. 4(c) and (f)), absorption in the c-Si solar cell is clearly higher in the energy range where the AM1.5G spectrum has its maximum.

We can also see that in the high-energy region, the increase of σ gives a clear absorption enhancement, but only a minor change of the spectral contribution to the J_{SC} . This is because the number of photons available in this part of the solar spectrum is small.

4. Randomly rough textures and the Lambertian Limit of absorption

The Lambertian Limit [32] of absorption is often taken as a fundamental benchmark for solar cells. In this work, we calculate it using the formalism derived in [33] and extended in [34]. In general, the total absorption in a structure with the Lambertian Scatterer, assuming a perfect back reflector, is given by

$$A_{\text{T}} = \frac{(1 - R_{\text{ext}})(1 - T^+T^-)}{1 - R_{\text{f}}T^+T^-}, \quad (2)$$

where T^+ is the transmittance through the active layer for light propagating from the front surface to the back reflector and T^- is the transmittance through the active layer for light reflected from the back surface. Finally, R_{f} is the part of light trapped in the active layer by total internal reflection and R_{ext} is the reflectance at the initial interface. The product of T^+T^- depends on the structure, and the value of R_{f} depends on the dimensionality of the optical problem. For a one-dimensional structure with a rough interface at the top and a flat back reflector, T^+T^- and R_{f} are given by

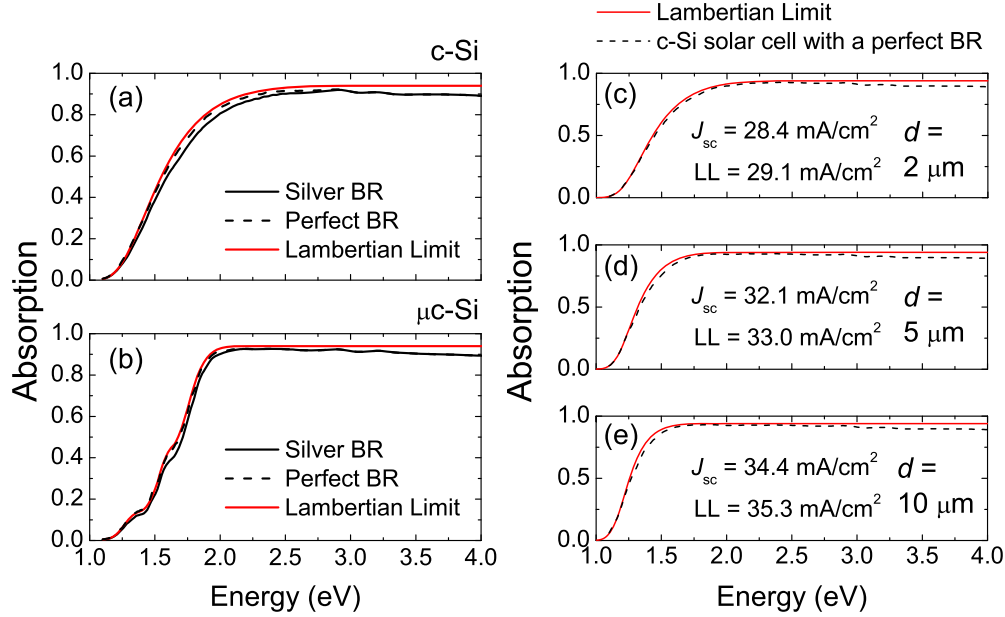


Fig. 5. Left: absorption in c-Si (a) and μ c-Si (b) solar cells with the optimized rough ARC/Si interface ($\sigma = 300$ nm, $l_c = 160$ nm) and an absorbing layer of $1 \mu\text{m}$, along with the corresponding Lambertian Limit. Both silver and perfect back reflectors (BR) were considered. Right: absorption in c-Si solar cells with rough ARC/Si interface ($\sigma = 300$ nm, $l_c = 160$ nm), a perfect back reflector (BR), and an absorbing layer of thickness $d = 2 \mu\text{m}$ (c), $5 \mu\text{m}$ (d), and $10 \mu\text{m}$ (e), along with the corresponding Lambertian Limit.

$$T^+T^- = \frac{\int_{-\pi/2}^{\pi/2} e^{-2\alpha d/\cos(\theta)} \cos(\theta) d\theta}{\int_{-\pi/2}^{\pi/2} \cos(\theta) d\theta}, \quad (3)$$

$$R_f = 1 - 1/n. \quad (4)$$

where d is the thickness of the active layer, α is the absorption coefficient, θ is the scattering angle, and n is the refractive index of the active layer [34].

In Fig. 5(a) and (b), we show the absorption calculated for c-Si and μ c-Si solar cells with the optimized rough ARC/Si interface ($\sigma = 300$ nm, $l_c = 160$ nm) and an absorbing layer of $1 \mu\text{m}$, along with the corresponding Lambertian Limit. Reflection losses at the Air/ARC interface were included in the Lambertian Limit to obtain a fair comparison. It should be noticed that, since the Lambertian Limit assumes no reflection losses at the back, we have also considered structures with a perfect mirror instead of silver. This allows to estimate the losses caused by a non-ideal back reflector.

In both cases, absorption in the structure with the optimized roughness and a perfect back reflector approaches the theoretical limit for a wide energy range. Small discrepancies can be seen only in the high energy region, where the effective wavelength in silicon is small comparing to the correlation length of the roughness, and the anti-reflection action of the rough interface becomes less effective. In this region, however, solar photon flux is small anyway. Similar results were obtained for the rough interface with the same parameters ($\sigma = 300$ nm, $l_c = 160$ nm) and an absorbing layer of $2 \mu\text{m}$, $5 \mu\text{m}$, and $10 \mu\text{m}$. The results for c-Si are shown

Table 1. Short-circuit current densities calculated for $1\ \mu\text{m}$ thick c-Si and $\mu\text{c-Si}$ solar cells, with either silver or perfect back reflectors (BR), together with the values corresponding to the Lambertian Limit. The parameters of the rough interface are: $\sigma = 300\ \text{nm}$, $l_c = 160\ \text{nm}$.

	silver BR	perfect BR	Lambertian Limit
c-Si	23.9 mA/cm ²	24.9 mA/cm ²	25.5 mA/cm ²
$\mu\text{c-Si}$	22.8 mA/cm ²	23.5 mA/cm ²	23.9 mA/cm ²

in Fig. 5(c), (d) and (e).

The short-circuit current densities calculated for the solar cells with an absorbing layer of $1\ \mu\text{m}$ are given in Tab. 1. The J_{SC} for the structures with an ideal back reflector are very close to those corresponding to the Lambertian Limit.

So far we considered one-dimensional structures. Yet, because the scattering properties of rough interfaces are isotropic, absorption in the two-dimensional structure with an optimized rough interface is expected to approach the corresponding two-dimensional Lambertian Limit. Thus, the general conclusions of this work concerning the optimal values of roughness parameters to approach the ultimate limits for light trapping are expected to be valid for real 2D interfaces.

5. Optical properties of randomly rough interfaces

Optical properties of rough interfaces can give insight into the light trapping mechanisms in thin-film solar cells. Therefore, we focus on the rough interface, sketched in the inset of Fig. 6, between the transparent medium with refractive index equal to $n_{\text{ARC}}=1.65$ and crystalline silicon [25] with complex refractive index. Following [35], we describe the light transmitted into the active layer by: 1) Angular Intensity Distribution (AID), which is the intensity of scattered light as a function of the scattering angle; 2) haze, which is the ratio of the intensity of scattered

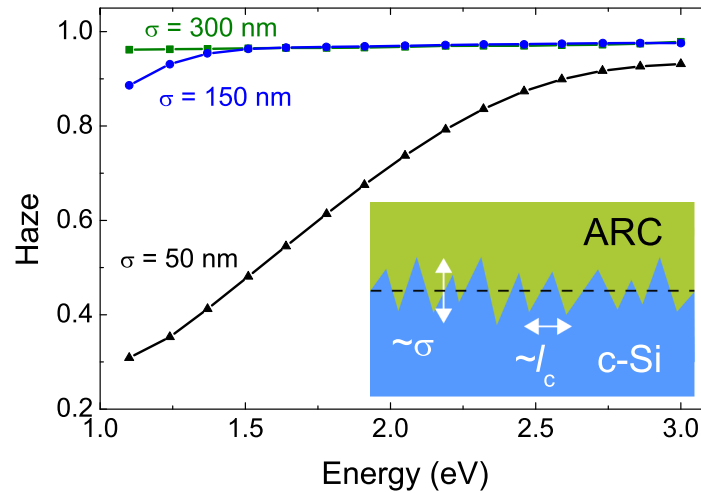


Fig. 6. Haze of transmitted light as a function of energy for increasing RMS deviation of height σ , calculated for the rough interface sketched in the inset. Both anti-reflection coating (ARC) and c-Si layer are assumed to be semi-infinite. Each point is taken as an average of 500 rough surface realizations. The lateral correlation length is equal to $l_c = 160\ \text{nm}$.

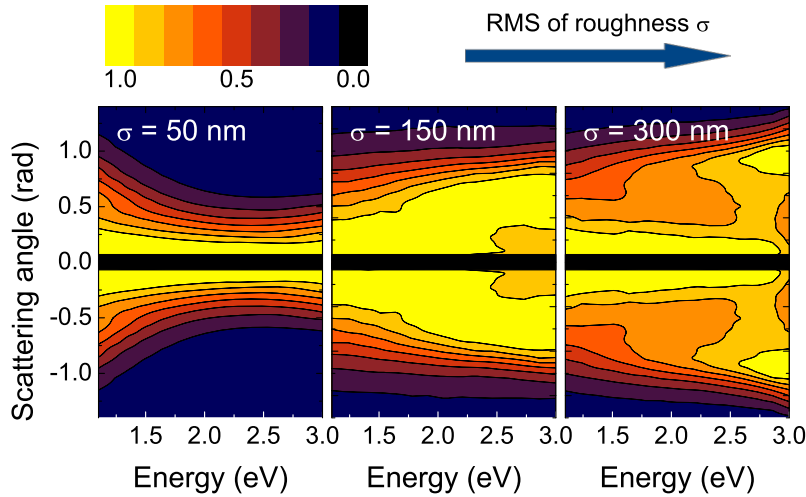


Fig. 7. AID of transmitted light as a function of energy for increasing RMS deviation of height σ , calculated for the rough ARC/c-Si interface. The AID is taken as an average of 500 rough surface realizations. The black rectangles denote the specular part of transmitted light (i.e., the light propagating within the cone between -1.5° and 1.5°). The lateral correlation length is equal to $l_c = 160\text{nm}$.

light to the total intensity of transmitted light (scattered and specular). We consider the light to be specular if it is propagating within the cone between -1.5° and 1.5° . Both AID and haze are calculated just below the rough interface, and are taken as an average of 500 rough surface realizations. Finally, we study the AID and the haze in the energy range between 1.1 and 3.0 eV. For energies higher than 3.0 eV, crystalline silicon absorbs very well, but the solar photon flux in this part of the spectrum is small.

In Fig. 6, we show the haze as a function of energy for increasing σ at fixed $l_c = 160\text{nm}$. For modest RMS ($\sigma = 50\text{nm}$), the haze increases steadily with the energy, from 0.3 in the region close to the energy band-gap, up to 0.9 for energies higher than 2.5 eV. The hazes for $\sigma = 150\text{nm}$ and $\sigma = 300\text{nm}$ are identical, except the low energy region, where a small discrepancy can be observed. Indeed, Fig. 3 shows that J_{SC} saturates above $\sigma = 150\text{nm}$. Therefore, changes in haze observed for large σ should be minor. Finally, at $\sigma = 300\text{nm}$, more than 90% of the incident light is diffused, regardless of energy.

AID as a function of energy at three different values of σ and at fixed $l_c = 160\text{nm}$ is shown in Fig. 7. When increasing σ , the intensity of light scattered at large angles is also increased, and the shape of the AID becomes less regular, particularly in the high energy region. This can be clearly seen in the cross-sections of the AID at two fixed energies ($E = 1.24\text{eV}$ and $E = 2.86\text{eV}$), shown in Fig. 8, where the AID is compared with a cosine distribution corresponding to the Lambertian Limit.

The AID at low energy, shown in Fig. 8(a), is narrower than the Lambertian distribution. It can be explained by the fact that the AID is calculated after the light has passed through the rough interface. At this point, part of the light has been already absorbed in the roughness, and, as was pointed out in [33], the light propagating in the device is being concentrated in the direction normal to the surface.

The AID at high energy, shown in Fig. 8(b), exhibits two symmetrical peaks at large σ ($\sigma = 150\text{nm}$, $\sigma = 300\text{nm}$). These peaks shift to smaller angles when energy or σ is decreased, which is in agreement with the behaviour expected from Fabry-Pérot oscillations in a thin film.

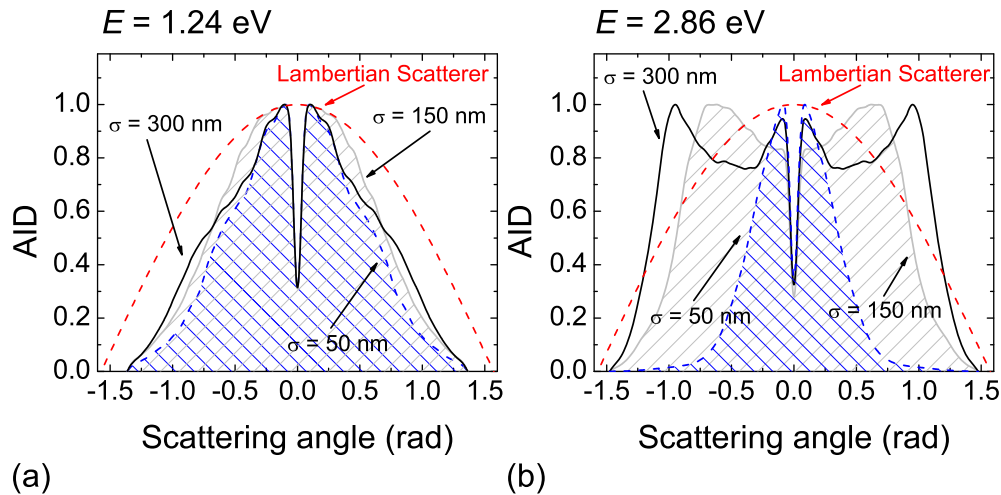


Fig. 8. AID of transmitted light at (a) $E = 1.24\text{ eV}$ and (b) $E = 2.86\text{ eV}$, calculated at three values of RMS deviation of height σ . The results are compared with the cosine distribution corresponding to the Lambertian Limit. Lateral correlation length is equal to $l_c = 160\text{ nm}$.

Therefore, we attribute the peaks to a constructive interference in the rough interface. Similar symmetrical peaks were observed in experimental studies of random textures, e.g., in AID of the light reflected from a rough monocrystalline silicon film [36] or in AID of the light transmitted through a rough air/glass interface [37]. Taking this irregular shape of the AID, it is important to note that in a high energy range and for a large σ , absorption very close to the corresponding Lambertian Limit is achieved for the interface with AID different from the cosine distribution of the Lambertian Scatterer.

6. Hybrid texture

Thus far we have seen that rough interfaces perform very well from the optical point of view. It has been pointed out [38, 39], however, that large and sharp surface features may worsen the electrical properties of a solar cell. To address this problem, we extend the idea of a modulated surface texture [40], and study a combination of a rough interface and a diffraction grating. We show that such a hybrid interface allows to obtain a strong absorption enhancement using a rough interface with a modest feature size. This approach is in line with recent findings demonstrating the benefits of joining ordered and disordered photonic structures. In this regard, possible light trapping schemes are realized either by introducing a certain amount of disorder into an ordered system (or the opposite) [34, 41], or by using separate ordered and disordered structures acting together [10]. Moreover, combining rough textures with different statistical properties has been also explored [42].

The structure under investigation is sketched in Fig. 1(b). This is a $1\ \mu\text{m}$ thick c-Si solar cell similar to the structure considered previously, except that the rough interface has been replaced by a combination of a rough interface and a diffraction grating. The grating has the period a , the width of the etched region b , and the etching depth h . The optimal parameters for $1\ \mu\text{m}$ c-Si solar cell are: $a = 600\text{ nm}$, $b = 180\text{ nm}$, $h = 240\text{ nm}$ [3]. Moreover, we took a rough interface with $\sigma = 80\text{ nm}$, $l_c = 60\text{ nm}$. According to the data presented in [42], this small and sharp features should assure good electrical properties of the interface, by avoiding cracks that form when the surface features are not small enough.

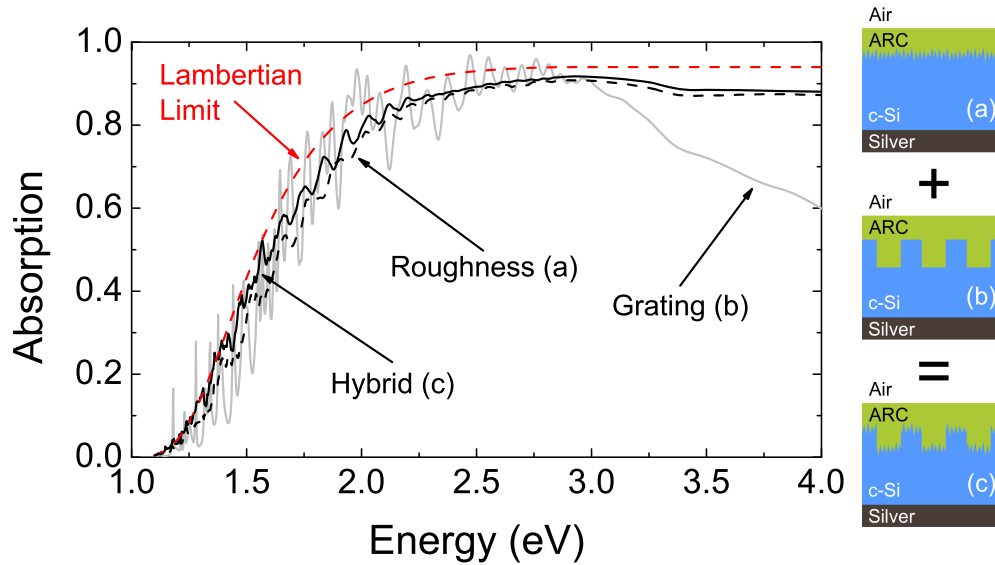


Fig. 9. Absorption in $1\ \mu\text{m}$ thick c-Si solar cells with (a) the rough interface with a modest spatial features ($\sigma = 80\ \text{nm}$, $l_c = 60\ \text{nm}$), (b) the optimal diffraction grating ($a = 600\ \text{nm}$, $b = 180\ \text{nm}$, $h = 240\ \text{nm}$), and (c) the hybrid interface. The structures are sketched on the right. The results are compared with the corresponding Lambertian Limit of absorption.

Table 2. Short-circuit current density J_{SC} and its relative enhancement for a $1\ \mu\text{m}$ thick c-Si solar cell with the optimal diffraction grating ($a = 600\ \text{nm}$, $b = 180\ \text{nm}$, $h = 240\ \text{nm}$), the rough interface with a modest spatial features ($\sigma = 80\ \text{nm}$, $l_c = 60\ \text{nm}$), the hybrid interface, and the optimized rough interface ($\sigma = 300\ \text{nm}$, $l_c = 160\ \text{nm}$), compared with the J_{SC} corresponding to the Lambertian Limit. Relative enhancement of the J_{SC} was calculated with respect to the structure with a flat ARC/Si interface.

structure	J_{SC} (mA/cm^2)	relative enhancement
reference cell (flat ARC/Si interface)	16.5	1.00
rough interface ($\sigma = 80\ \text{nm}$, $l_c = 60\ \text{nm}$)	22.2	1.35
optimal grating	22.6	1.37
hybrid interface	23.7	1.44
optimal roughness ($\sigma = 300\ \text{nm}$, $l_c = 160\ \text{nm}$)	23.9	1.45
Lambertian Limit	25.5	1.55

Figure 9 shows the absorption calculated for $1\ \mu\text{m}$ thick c-Si solar cells with a rough interface (a), a diffraction grating (b), and a combination of both (c). Adding the diffraction grating to the rough interface clearly increases the absorption, resulting in a redshift of the whole spectrum. Nevertheless, absorption in the structure with the hybrid interface does not reveal the spectral features coming from the grating. This is consistent with the results reported in [10], where spectral features corresponding to a photonic crystal are smoothed when a randomly rough surface is added. The values of J_{SC} for the structures considered here are summarized in Tab. 2. The structure with the hybrid interface clearly outperforms that with the optimized diffraction grating, as well as the one with the rough interface ($\sigma = 80\ \text{nm}$, $l_c = 60\ \text{nm}$). As a result, the hybrid interface allows to significantly reduce σ ; indeed, $J_{\text{SC}} = 23.7\ \text{mA}/\text{cm}^2$ has been obtained

for $\sigma = 80$ nm, compared to $\sigma = 200$ nm, which is necessary to achieve that high J_{SC} in the corresponding structure with a rough interface. Thus, use of a hybrid interface might allow to achieve Lambertian light trapping even with relatively small values of σ that correspond to common (Asahi-U and Neuchâtel) substrates, as shown previously in Fig. 2.

These findings show that a hybrid interface is a promising approach to achieve broad-band absorption enhancement with shallow roughness. As a final remark, we stress that the scattering properties of a hybrid interface are no longer isotropic. Thus, the connection between 1D model and the optical properties of 2D system in the case of a hybrid interface is not as straightforward as it is for isotropic rough interfaces.

7. Conclusions

In this contribution, we have used a simple but accurate model of Gaussian roughness to study light-trapping in thin-film solar cells with rough interfaces. We have considered solar cells made of different materials (c-Si and μ c-Si), showing that without light trapping, absorption in the structure is mainly determined by the *nature* (direct/indirect) of the energy band gap, while for efficient light trapping, the band gap *size* is the most important.

We have demonstrated that short-circuit current density in c-Si and μ c-Si solar cells with optimized roughness is very close to the J_{SC} corresponding to the Lambertian Limit. Since the optical properties of randomly rough interfaces are isotropic, we expect that 2D structures with optimized roughness will approach the 2D Lambertian Limit. This, for an absorbing layer of 1 μ m, would give J_{SC} close to 31.9 mA/cm² for c-Si solar cell and 29.7 mA/cm² for μ c-Si solar cell. Moreover, the optimal parameters of the roughness are expected to be the same for 1D model and for real 2D substrates. We stress that the values of J_{SC} given here include reflection losses at the Air/ARC interface. Assuming perfect anti-reflection action, we calculate J_{SC} in a structure with the 2D Lambertian Scatterer to be 33.9 mA/cm² (c-Si) and 31.6 mA/cm² (μ c-Si).

The concept of a hybrid interface, which is a combination of a randomly rough interface and a diffraction grating, allowed to achieve significant absorption enhancement with a shallow roughness. The purpose in reducing the vertical size of the roughness was to assure good electrical properties of a rough interface. This study confirms that a combination of ordered and disordered photonic structures may be beneficial for light trapping in thin-film solar cells, in line with recent findings documented in the literature for other kinds of systems [7, 10, 34, 41].

Finally, the model of roughness considered here is able to predict the scattering properties of realistic rough surface topographies, such as Neuchâtel and Asahi-U substrates. In view of recent progress in fabrication of thin monocrystalline silicon films and of the possibility of using nanoimprint lithography, structures presented in this work are compatible with present-day technologies and can be realised in practice on large areas and at low cost.

Acknowledgments

The authors are grateful to Franz-Joseph Haug, Olindo Isabella, and Thomas Lanz for helpful discussions. This work was supported by the EU through Marie Curie Action FP7-PEOPLE-2010-ITN Project No. 264687 "PROPHET" and Fondazione Cariplo project 2010-0523 "Nanophotonics for thin-film photovoltaics". We also acknowledge CINECA/CASPUR project "Disorder" under the ISCRA initiative, for the availability of high performance computing resources and support.